

phys. stat. sol. (a) **170**, 349 (1998)

Subject classification: 78.66.Bz; 78.20.Bh; S4

## **Local-Field Effects at Crystalline Surfaces: Electron Energy Loss from Ordered Arrays of Spheres**

C. I. MENDOZA (a), R. G. BARRERA (a), and R. FUCHS (b)

(a) *Instituto de Física, Universidad Nacional Autónoma de México, Apartado Postal 20-364, 01000 México Distrito Federal, México*

(b) *Ames Laboratory and Department of Physics and Astronomy, Iowa State University, Ames, Iowa 50011, USA*

(Received July 31, 1998)

Local-field effects at crystalline surfaces are analyzed on a classical system consistent of ordered arrays of polarizable spheres. A theory for the energy loss of fast electrons traveling parallel to these arrays is presented. A spectral representation of the surface response function is used to calculate this energy loss. The poles and weights in this representation are determined through the eigenvalues and eigenvectors of an interaction matrix which takes into account the quasi-static electromagnetic fields to an arbitrary multipolar order. We apply the theory to calculate the energy-loss spectra for cubic arrays of aluminum spheres embedded in vacuum and compare the results with those obtained using a dielectric continuum model.

### **1. Introduction**

The effects of the local field (LF) in the optical properties of crystalline surfaces has been a topic of continuous research during the last decades [1]. The local field at a point is related to the polarization properties of matter and is defined as the sum of the applied plus the induced field, the latter being the field produced by the induced-charge and -current densities. Therefore, the origin of the LF is the two-body electron-electron interaction, and since the source are charge and current densities it is also a many-body effect. The inclusion of LF effects in the calculation of the dielectric response of matter has a long history. For example, in the case of a system of isolated isotropic molecules located at random, a mean-field approach yields the celebrated Clausius-Mossotti relation. By using different approaches [1], it has become clear that the calculation of the LF effect is a rather complicated computational process, and it requires, as a starting point, the microscopic dielectric response for all wavevectors on the reciprocal space; a quantity difficult to calculate. In the case of the bulk, the above procedure has been tested in some wide bandgap materials and semiconductors, but in the case of a crystalline surface this has not been possible and alternative approaches had to be devised. Also, in other schemes like the time-dependent Hartree approximation (TDH) or in the time-dependent local-density approximation (TDLDA) part of the LF effects were recently introduced through the use of the dipolium model [2]. In this model the crystal is thought to be composed by cells with an effective polarizability and these cells interact with each other through the dipole-dipole interaction. It was shown that in the case of cubic semiconductors like Si and Ge, the surface LF effects were not negligible and their sole inclusion was able to reproduce fairly well

the profile of the reflectance anisotropy spectra (RAS) [2], [3]. The ideas behind the use of the dipolium model have been extended by Mochán and Tarriba [4] to the case of metallic surfaces by devising, what is now known as the ‘Swiss-cheese’ model. In this model the polarizable ion cores are regarded as spherical ‘holes’ within a homogeneous electron gas which mimics the s-p electrons. This model has been successfully applied to the calculation of the RAS spectra of the (100) face of Ag and Au [4], [5]. The use of either the dipolium or the ‘Swiss-cheese’ model have stressed the fact that, in essence, the LF effects are not a pure quantum-mechanical effect. The problem of the LF effect at surfaces appears also in classical systems, inheriting some of the main complexities present in the quantum-mechanical ones. Due to the importance of the LF effects at surfaces, it is an important ingredient in the calculation of electron energy-loss spectra of high energy electrons [6], a technique that is becoming an important tool for structural analysis of surfaces [7]. Here we will present the calculation of the electron energy loss of electrons passing above an ordered array of polarizable spheres including local-field effects through a multipolar expansion. That is the reason why we call this model the multipolium. The effect of the induced multipoles beyond the dipole is displayed and we compare the results with those obtained using a dielectric continuum model.

## 2. Formalism

Let us consider a cubic array of identical polarizable spheres of radius  $a$  and a local dielectric function  $\epsilon_s(\omega)$  occupying a slab-shaped portion of the region of space  $z < 0$ , as shown in Fig. 1. A fast electron is traveling at speed  $v_I$  on a rectilinear trajectory along the  $y$ -axis and at a distance  $z_0$  above the surface of the slab. Its coordinates at time  $t$  are given by  $(x_0, v_I t, z_0)$ . The array is tilted by an angle  $\phi$  with respect to the  $x$ -axis (see Fig. 1). Our aim is to calculate the energy lost by the electron as it travels above the system of spheres in the quasi-static approximation.

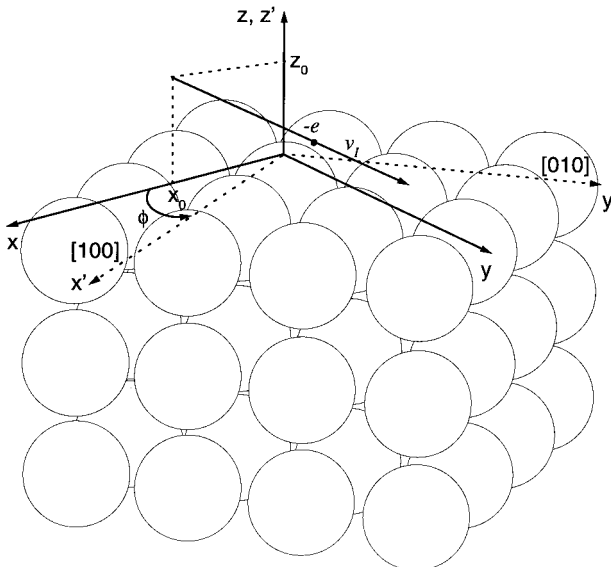


Fig. 1. An electron with charge  $-e$  moves with velocity  $\mathbf{v}_I = v_I \mathbf{e}_y$  parallel to an ordered array of spheres. The direction [100] of the lattice makes an angle  $\phi$  with respect to the  $x$ -axis

In order to perform the calculation of the energy loss it is convenient to work with Fourier transforms with respect to time and two of the spatial variables. For example, in the region  $z < z_0$ , the time Fourier transform of the external potential produced by external charges located at  $z \geq z_0$  satisfies the Laplace equation and can be written as [8]

$$\phi^{\text{ext}}(\mathbf{q}, z; \omega) = \int \frac{d^2 Q}{(2\pi)^2} \phi^{\text{ext}}(\mathbf{Q}, \omega) e^{i\mathbf{Q} \cdot \mathbf{q} + Qz}; \quad z < z_0, \quad (1)$$

where  $\mathbf{q} = (x, y)$ , and  $\omega$  and  $\mathbf{Q} = (Q_x, Q_y)$  are the frequency and the two-dimensional wave vector, respectively. The magnitude of  $\mathbf{Q}$  is denoted by  $Q \equiv |\mathbf{Q}|$ . A similar expression is satisfied by the induced potential in the region  $z > 0$ .

We assume a linear relationship between the induced and external potentials which can be written, for systems with crystalline periodicity parallel to the interface, as

$$\phi^{\text{ind}}(\mathbf{Q}, \omega) = -\sum_{\mathbf{G}} g(\mathbf{Q}, \mathbf{Q} + \mathbf{G}; \omega) \phi^{\text{ext}}(\mathbf{Q} + \mathbf{G}, \omega), \quad (2)$$

where  $\mathbf{G}$  is the two-dimensional reciprocal lattice vector corresponding to the crystal lattice.

The energy loss  $dW$  of the electron as it moves a distance  $dy$  is given by

$$\frac{dW}{dy} = -e \left. \frac{\partial \phi^{\text{ind}}(x, y, z, t)}{\partial y} \right|_{x=x_0, y=v_1 t, z=z_0}, \quad (3)$$

where  $-e$  is the charge of the electron. For our system it is found that the energy loss contains terms that oscillate in time, which correspond to a time-dependent energy loss [9]. Since we are interested only in the time average of the energy loss and performing, for simplicity, a lateral scanning of the electron beam, then only the term with  $\mathbf{G} = 0$  contributes to the averaged energy loss and we can write

$$\left\langle \frac{dW}{dy} \right\rangle_{t, x_0} = \frac{e^2}{\pi v_1^2} \int_0^\infty \omega d\omega \int_{-\infty}^\infty dQ_x \frac{e^{-2Qz_0}}{Q} \text{Im} g(\mathbf{Q}; \omega), \quad (4)$$

where  $\langle \dots \rangle_{t, x_0}$  means time and lateral average,  $g(\mathbf{Q}, \omega) \equiv g(\mathbf{Q}, \mathbf{Q}; \omega)$ , and  $\mathbf{Q} = \left( Q_x, \frac{\omega}{v_1} \right)$ .

We define  $d^2P/dl dE$ , the probability per unit path length, per unit energy, for an electron to be scattered with energy loss  $E = \hbar\omega$ , through

$$\left\langle \frac{dW}{dy} \right\rangle_{t, x_0} = \int_0^\infty dE E \frac{d^2P}{dl dE} = (a_0 E_1)^{-1} \int_0^\infty dE E \Xi(E), \quad (5)$$

where the dimensionless quantity  $\Xi(E)$  is called the energy-loss probability function. Here  $a_0$  is the Bohr radius and  $E_1$  is the electron incident energy. By combining Eqs. (4) and (5) one can write

$$\Xi(E) = \frac{1}{2\pi} \int_{-\infty}^{+\infty} dQ_x \frac{e^{-2Qz_0}}{Q} \text{Im} g(\mathbf{Q}, \omega). \quad (6)$$

The response function  $g(\mathbf{Q}, \omega)$  carries information about the interaction among the spheres. Following [8] the calculation of  $g(\mathbf{Q}, \omega)$  is performed to all multipolar orders

and expressed as a spectral representation in the following form:

$$g(\mathbf{Q}, \omega) = -\frac{1}{2} \sum_s \frac{D_s(\mathbf{Q})}{u(\omega) - n_s(\mathbf{Q})}, \quad (7)$$

where

$$u(\omega) = -\frac{1}{\varepsilon_s(\omega) - 1} \quad (8)$$

is the spectral variable, which depends on the dielectric properties of the material. The words *spectral representation* mean that  $g(\mathbf{Q}, \omega)$  is expressed as a sum of terms with simple poles, where the poles located at  $u(\omega_s) = n_s(\mathbf{Q})$  yield the dispersion relations  $\omega_s(\mathbf{Q})$  of the polarization normal modes of the system, and the residues  $D_s(\mathbf{Q})$  give the strength of the coupling of these modes with the external potential. Both  $n_s(\mathbf{Q})$  and  $D_s(\mathbf{Q})$  depend only on the geometry of the system and not on the dielectric properties of the materials. The procedure for the calculation of  $n_s(\mathbf{Q})$  and  $D_s(\mathbf{Q})$  can be found in [9]. It turns out that the  $n_s(\mathbf{Q})$  correspond to the eigenvalues of an interaction matrix

$$H_{lmi}^{l'm'j}(\mathbf{Q}) = \frac{l}{2l+1} \delta_{ll'} \delta_{mm'} \delta_{ij} + \frac{1}{4\pi} \sqrt{ll'} a^{l+l'+1} B_{lmi}^{l'm'j} e^{i\mathbf{Q} \cdot (\mathbf{e}_j - \mathbf{e}_i)} (1 - \delta_{ij}). \quad (9)$$

An expression for the quantities  $B_{lmi}^{l'm'j}$  appears in [6]. Notice that the location of the spheres is completely arbitrary in the above expressions, so they can be used for either an ordered or disordered system.

Then, one can show (see [9]) that the strengths  $D_s(\mathbf{Q})$  can be written as

$$D_s(\mathbf{Q}) = \sum_{lmi, l'm'j} A_{Q, lmi} U_{lmi, s} U_{s, l'm'j}^{-1} A_{l'm'j, Q}. \quad (10)$$

Here,  $U_{lmi, s}$  is the unitary matrix which diagonalizes the matrix  $H_{lmi}^{l'm'j}$  and

$$A_{l'm'j, Q} = \frac{\sqrt{4\pi}}{L} (-i^{m'}) e^{-im'\eta} \sqrt{\frac{la^{2l+1}}{(2l'+1)(l'+m')!(l'-m')!}} Q^{l'-1/2} e^{Qz_i}, \quad (11)$$

with  $A_{Q, lmi} = (A_{lmi, Q})^*$ ,  $\eta$  the angle of  $\mathbf{Q}$  with respect to the  $x$ -axis, and  $L (\rightarrow \infty)$  the size of the system in the  $x$  and  $y$  directions. These results are exact within the above-mentioned assumptions, and Eqs. (6) to (11) establish a well-defined procedure for the calculation of  $\Xi(E)$ .

### 3. Results

In this section we present numerical solutions for  $\Xi(E)$  for a system of aluminum spheres in vacuum. The dielectric response of aluminum is modeled by a Drude dielectric function

$$\varepsilon_s(\omega) = 1 - \frac{\omega_p^2}{\omega(\omega + i/\tau)}, \quad (12)$$

where  $\omega_p$  is the plasma frequency and  $\tau$  the relaxation time. In the results presented below the Drude parameters for aluminum have been taken as  $\hbar\omega_p = 16$  eV and  $\omega_p\tau = 100$ . Also, we have fixed  $E_1 = 100$  keV, which corresponds to the typical incident energies for electrons produced in a scanning transmission electron microscope, and we

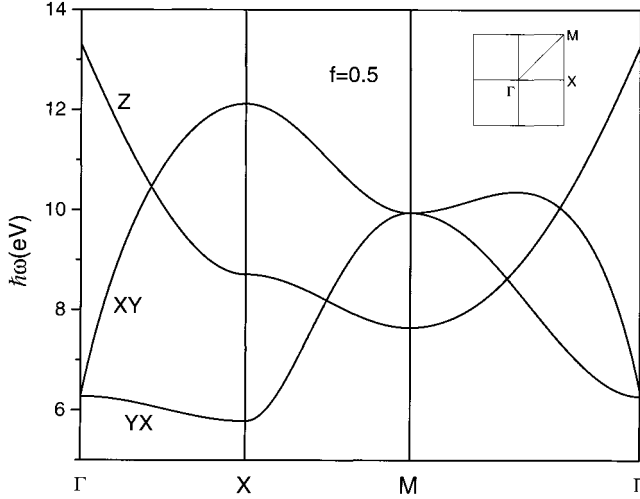


Fig. 2. Dispersion relations of the three normal modes of the electric field in a single layer of spheres with  $L_{\max} = 1$ . The filling fraction is  $f = 0.5$

have chosen  $a = 2.5$  nm and  $z_0 = 1$  nm. We will show results for systems with different number  $n_z$  of layers, and for different values of the filling fraction of the spheres  $f$ , the maximum multipolar order considered in the calculation  $L_{\max}$ , and the angle  $\phi$  which the electron trajectory makes with the  $[010]$  direction of the cubic lattice.

First, we present results for a single layer of spheres in a square lattice taking  $L_{\max} = 1$ , which corresponds to the dipolar approximation. In Fig. 2 we plot the dispersion relation  $\hbar\omega_s(\mathbf{Q})$  of the three ( $s = 1, 2, 3$ ) normal modes of the electric field in the layer. We have chosen  $f = 0.5$  and a definite trajectory in reciprocal space. The two-dimensional periodicity in the  $xy$  plane introduces a dependence of the dispersion relations  $\hbar\omega_s(\mathbf{Q})$  on the direction of  $\mathbf{Q}$ . Each of these modes has a particular direction of polarization. One is along the  $z$  direction, labeled  $Z$ , and two modes, labeled  $XY$  and  $YX$ , are linearly polarized in the  $xy$  plane and are orthogonal to each other. There is no interaction between the different directions of polarization, so the modes preserve their character when they cross.

In Fig. 3 we have plotted  $\Xi(E)$  for  $f = 0.15$  and  $0.5$ ,  $L_{\max} = 1$ , and three different angles,  $\phi = 0^\circ, 30^\circ$  and  $45^\circ$ . As a comparison we also show the corresponding functions  $\Xi(E)$  given by the Maxwell Garnett theory (MGT). In this effective-medium theory the inhomogeneous system is regarded as a homogeneous slab of thickness  $d = a(4\pi/3f)^{1/3}$  with an effective dielectric response  $\epsilon_{\text{MG}}(\omega)$ , given by [10]

$$\epsilon_{\text{MG}}(\omega) = \frac{u(\omega) - (1 + 2f)/3}{u(\omega) - (1 - f)/3}. \quad (13)$$

This theory corresponds to a mean-field dipolar approximation which means that the polarized spheres interact only through their induced average dipole moment [11]. On the other hand, the surface response function  $g(\mathbf{Q}, \omega)$  for a homogeneous slab of thickness  $d$  with a local dielectric response  $\epsilon(\omega)$  is given by [12]

$$g(\mathbf{Q}, \omega) = \frac{[\epsilon^2(\omega) - 1] (e^{Qd} - e^{-Qd})}{F_-(\mathbf{Q}, \omega) F_+(\mathbf{Q}, \omega)}, \quad (14)$$

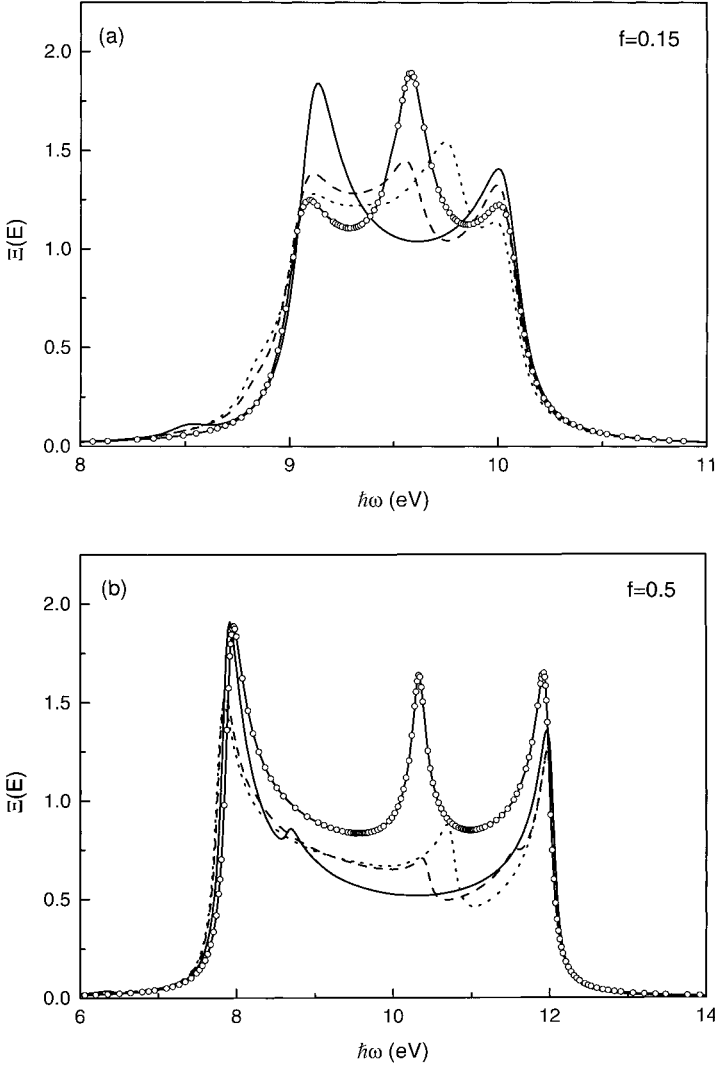


Fig. 3. a) Energy-loss probability function  $\Xi(E)$  as a function of the energy loss  $E = \hbar\omega$  for a single layer of spheres with a filling fraction  $f = 0.15$  and  $L_{\max} = 1$ . Three different angles of the electron trajectory with respect to the  $[010]$  axis of the array of spheres were chosen:  $\phi = 0^\circ$  (solid line),  $30^\circ$  (dashed line) and  $45^\circ$  (dotted line). The open circles represent the corresponding result as given by the Maxwell Garnett theory with  $d = 7.58$  nm. b) The same as in a) but for  $f = 0.5$  and  $d = 5.07$  nm

where

$$F_{\pm}(\mathbf{Q}, \omega) = \epsilon(\omega) (e^{Qd/2} \pm e^{-Qd/2}) + e^{Qd/2} \mp e^{-Qd/2}. \quad (15)$$

In the MGT the slab has no structure in the  $xy$  plane, so  $g_{\text{MG}}(\mathbf{Q}, \omega)$  does not depend on the direction of  $\mathbf{Q}$  and  $\Xi(E)$  is independent of the trajectory angle  $\phi$ .

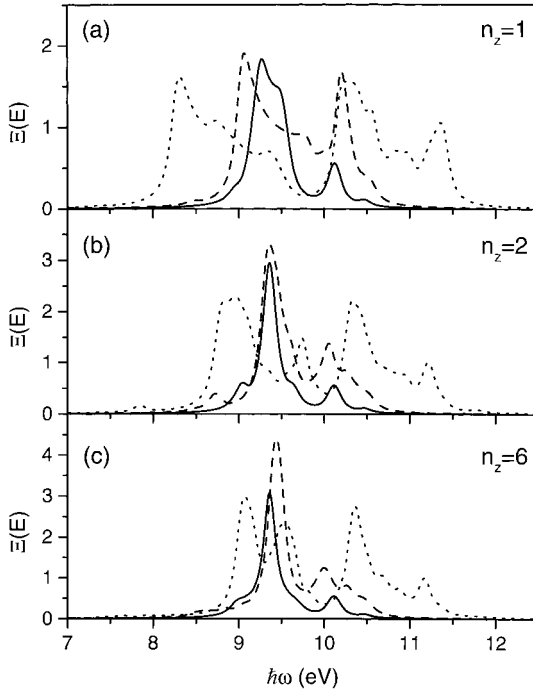


Fig. 4. a) Energy-loss probability function  $\Xi(E)$  as a function of the energy loss  $E = \hbar\omega$  for slabs made of  $n_z = 1$  layers of spheres and with filling fractions  $f = 0.065, 0.15,$  and  $0.3$ . The maximum multipolar order,  $L_{\max}$ , was chosen in order to achieve multipolar convergence. For all curves  $\phi = 0^\circ$ . The solid line corresponds to  $f = 0.065$  with  $L_{\max} = 3$ , the dashed line to  $f = 0.15$  with  $L_{\max} = 3$ , and the dotted line to  $f = 0.3$  with  $L_{\max} = 8$ . b) The same as in (a) but with  $n_z = 2$ . c) The same as in (a) but with  $n_z = 6$

The inclusion of higher-order multipoles will give rise to a larger number of modes. In this case the analysis of the contribution of all different modes to  $\Xi(E)$  is more complicated, nevertheless, it turns out that as the number of modes increases the band of energies occu-

ried by the modes also increases until convergence is attained.

Now we consider a system composed of  $n_z$  layers of spheres with their centers located, as discussed above, in a cubic lattice. In Fig. 4 we show the spectra of  $\Xi(E)$  for systems with various values of  $n_z$  and  $f$ . The value of  $L_{\max}$  is chosen so that multipolar convergence is achieved. In Fig. 4a we plot  $\Xi(E)$  for  $n_z = 1$  and  $f = 0.065, 0.15$  and  $0.3$ . As it can be seen, the larger the filling fraction of the spheres, the higher the maximum multipolar order to be considered in the calculation to achieve convergence. In Figs. 4b and c we show the spectra of  $\Xi(E)$  for  $n_z = 2$  and  $6$ , respectively, and filling fractions  $f = 0.065, 0.15$  and  $0.3$ . In all these plots, the spectra with the largest number of layers correspond to the half-space limit.

#### 4. Summary

We presented a theory for the calculation of the energy-loss probability function for an electron traveling on a definite trajectory outside an ordered array of polarizable spheres confined to a slab-shaped region of space. The trajectory makes an arbitrary angle with respect to the symmetry directions of the array. The local field produced by the polarized spheres is calculated to all multipolar orders in the nonretarded limit.

The energy loss is given in terms of a surface response function  $g(\mathbf{Q}, \mathbf{Q} + \mathbf{G}; \omega)$  which is expressed as a spectral representation. Taking a time average and also an average over lateral positions of the trajectory, we find that only the  $\mathbf{G} = \mathbf{0}$  term survives, so the energy loss depends on the distance of the trajectory from the surface and on the trajectory angle, and a simpler response function  $g(\mathbf{Q}, \omega)$  can be used in the energy-loss calculation.

We apply our theory to an array of spheres with their centers placed on a cubic lattice, and present results for slabs containing 1 to 6 layers of aluminum spheres in vacuum.

We also show that a simplified theory, in which the layer of spheres is replaced by a slab filled with a homogeneous dielectric medium given by the Maxwell Garnett theory, gives energy-loss spectra that agree qualitatively with those found using the exact theory in the dipole approximation.

**Acknowledgements** Part of this work was done at the Cavendish Laboratory, Department of Physics, University of Cambridge. We are grateful to A. Howie, J. Rodenburg, and other members of the Microstructural Physics Group for their hospitality. R.G.B. acknowledges the financial support of Dirección General de Asuntos del Personal Académico of Universidad Nacional Autónoma de México through Grant No. IN-104297, and to Consejo Nacional de Ciencia y Tecnología through Grant No. 0075-PE. C.I.M. acknowledges the support of Dirección General de Intercambio Académico of Universidad Nacional Autónoma de México and Fundación UNAM, A.C. through “Reconocimiento a estudiantes distinguidos de la UNAM”. Ames Laboratory is operated for the U.S. Department of Energy by Iowa State University under Contract No. W-7405-Eng-82.

## References

- [1] W. L. MOCHÁN and R. G. BARRERA, *Phys. Rev. B* **32**, 4989 (1985), and references therein.
- [2] W. L. MOCHÁN and R. G. BARRERA, *Phys. Rev. Lett.* **55**, 1192 (1985).
- [3] W. L. MOCHÁN and R. G. BARRERA, *Phys. Rev. Lett.* **56**, 2221 (1986).
- [4] Y. BORENSZTEIN, W. L. MOCHÁN, J. TARRIBA, R. G. BARRERA, and A. TADJEDDINE, *Phys. Rev. Lett.* **71**, 2334 (1993).
- [5] W. L. MOCHÁN, R. G. BARRERA, Y. BORENSZTEIN, and A. TADJEDDINE, *Physica* **207A**, 334 (1994).
- [6] R. G. BARRERA and R. FUCHS, *Phys. Rev. B* **52**, 3256 (1995).
- [7] A. HOWIE and C. A. WALSH, *Microscop. Microanal.* **2**, 171 (1991).
- [8] R. FUCHS, C. I. MENDOZA, R. G. BARRERA, and J. L. CARRILLO, *Physica* **241A**, 29 (1997).
- [9] C. I. MENDOZA, R. G. BARRERA, and R. FUCHS, submitted to *Phys. Rev. B*.
- [10] J. C. MAXWELL GARNETT, *Phil. Trans. Roy. Soc.* **203**, 385 (1904).
- [11] R. G. BARRERA, G. MONSIVAIS, and W. L. MOCHÁN, *Phys. Rev. B* **38**, 5371 (1988).
- [12] P. M. ECHENIQUE and J. B. PENDRY, *J. Phys. C* **8**, 2936 (1975).